New Phytologist

Research

Parallel evolution of morphological and genomic selfing syndromes accompany the breakdown of heterostyly

Zhi-Hua Zeng[1,2], Li Zhong[1,2], Hua-Ying Sun[3], Zhi-Kun Wu[4], Xin Wang[1,2,5], Hong Wang[5], De-Zhu Li[1,5], Spencer C. H. Barrett[6] and Wei Zhou[1,5,7]

[1]Germplasm Bank of Wild Species, Yunnan Key Laboratory of Crop Wild Relatives Omics, Kunming Institute of Botany, Chinese Academy of Sciences, Kunming, Yunnan, 650201, China; [2]University of Chinese Academy of Sciences, Beijing, 100049, China; [3]School of Chinese Materia Medica, Yunnan University of Chinese Medicine, Kunming, Yunnan, 650500, China; [4]Department of Pharmacy, Guizhou University of Traditional Chinese Medicine, Guiyang, Guizhou, 550002, China; [5]CAS Key Laboratory for Plant Diversity and Biogeography of East Asia, Kunming Institute of Botany, Chinese Academy of Sciences, Kunming, Yunnan, 650201, China; [6]Department of Ecology and Evolutionary Biology, University of Toronto, Toronto, ON, M5S 3B2, Canada; [7]Lijiang Forest Biodiversity National Observation and Research Station, Kunming Institute of Botany, Chinese Academy of Sciences, Lijiang, Yunnan, 674100, China

Authors for correspondence:
Wei Zhou
Email: zhouwei@mail.kib.ac.cn

Spencer C. H. Barrett
Email: spencer.barrett@utoronto.ca

De-Zhu Li
Email: dzl@mail.kib.ac.cn

Received: *7 November 2023*
Accepted: *18 December 2023*

New Phytologist (2024)
doi: 10.1111/nph.19522

Key words: floral evolution, heterostyly, homostyly, mating systems, *Primula*, selfing syndromes.

Summary

- Evolutionary transitions from outcrossing to selfing in flowering plants have convergent morphological and genomic signatures and can involve parallel evolution within related lineages. Adaptive evolution of morphological traits is often assumed to evolve faster than nonadaptive features of the genomic selfing syndrome.
- We investigated phenotypic and genomic changes associated with transitions from distyly to homostyly in the *Primula oreodoxa* complex. We determined whether the transition to selfing occurred more than once and investigated stages in the evolution of morphological and genomic selfing syndromes using 22 floral traits and both nuclear and plastid genomic data from 25 populations.
- Two independent transitions were detected representing an earlier and a more recently derived selfing lineage. The older lineage exhibited classic features of the morphological and genomic selfing syndrome. Although features of both selfing syndromes were less developed in the younger selfing lineage, they exhibited parallel development with the older selfing lineage. This finding contrasts with the prediction that some genomic changes should lag behind adaptive changes to morphological traits.
- Our findings highlight the value of comparative studies on the timing and extent of transitions from outcrossing to selfing between related lineages for investigating the tempo of morphological and molecular evolution.

Introduction

In flowering plants, evolutionary transitions from outcrossing to predominant selfing are associated with a set of predictable changes in both morphological traits and genetic features of the genome. These convergent and parallel changes have been termed the 'morphological selfing syndrome' and the 'genomic selfing syndrome', respectively (Sicard & Lenhard, 2011; Cutter, 2019; Tsuchimatsu & Fujii, 2022; Zhang *et al.*, 2022). Species with moderate-to-high selfing rates often exhibit smaller flowers, a loss of herkogamy (stigma-anther separation), reduced pollen production and pollinator rewards (e.g. scent and nectar) compared with related outcrossing species and populations (Lloyd, 1965; Morgan & Barrett, 1989; Ritland & Ritland, 1989; Liao *et al.*, 2022; Zeng *et al.*, 2022). Concomitantly, persistent selfing usually results in changes in genetic parameters, including reduced heterozygosity and nucleotide diversity, increased linkage disequilibrium, accumulation of deleterious mutations and changes in gene expression (Charlesworth & Wright, 2001; Wright *et al.*, 2008; Glémin & Galtier, 2012; Barrett *et al.*, 2014; Shimizu & Tsuchimatsu, 2015; Zhang *et al.*, 2022). The evolution of morphological and genomic syndromes accompanying the transition from outcrossing to selfing can involve both adaptive and nonadaptive processes (Cutter, 2019; Rifkin *et al.*, 2019; Liao *et al.*, 2022; Tsuchimatsu & Fujii, 2022; Zhang *et al.*, 2022). However, determining the relative contributions of positive selection vs genetic drift underpinning morphological and genetic changes accompanying the evolution of selfing syndromes remains a challenge.

In animal-pollinated species, morphological features of the selfing syndrome have often been interpreted as resulting from the phenotypic collapse of floral traits that previously functioned to attract pollinators and promote cross-pollination (Sicard & Lenhard, 2011; Kalisz *et al.*, 2012; Fornoni *et al.*, 2015). Shifts

© 2024 The Authors
New Phytologist © 2024 New Phytologist Foundation

to selfing should facilitate resource reallocation for fitness optimization, often over relatively short timescales (Foxe *et al.*, 2009; Guo *et al.*, 2009). Such relatively rapid morphological change implies that floral modifications have probably be driven by positive selection (Tsuchimatsu *et al.*, 2020), particularly as simulation models indicate that phenotypic changes under relaxed selection alone would take a much longer time and thus maybe unlikely (Glémin & Ronfort, 2013).

The genomic characteristics associated with shifts to selfing are often considered a maladaptive outcome leading to an evolutionary dead-end and extinction (Stebbins, 1957; Takebayashi & Morrell, 2001; Igic & Busch, 2013; Wright *et al.*, 2013; Barrett *et al.*, 2014). Population genetics theory indicates that in selfers, smaller effective population sizes (N_e) and stronger effects of linked selection (i.e. background selection and genetic hitchhiking) can result in the elevated accumulation of deleterious mutations causing 'mutational meltdown' in selfing genomes (Glémin & Galtier, 2012). Signatures of this process include high $\pi_N : \pi_S$ ratios, high $d_N : d_S$ ratios, and a low proportion of adaptive substitutions (α) (Slotte *et al.*, 2013; Arunkumar *et al.*, 2015; Chen *et al.*, 2017; Wang *et al.*, 2021). However, the effects of predominant selfing on the genome can often appear subtle and less easily detected than changes in morphological traits (Glémin & Galtier, 2012; Cutter, 2019). Indeed, some aspects of genomic decay (e.g. number of deleterious mutations per individual) resulting from relaxed selection and genetic drift are expected to involve much longer timescales compared with trait changes associated with the morphological selfing syndrome. However, the erosion of nucleotide diversity (π) and changes in heterozygosity are also likely to be more rapid.

Lack of empirical evidence for the genomic selfing syndrome in some lineages has often been attributed to the recent origin of selfing because of insufficient time for molecular signatures to be detected (Wright *et al.*, 2008; Escobar *et al.*, 2010; Ness *et al.*, 2012; Slotte *et al.*, 2013; Glémin & Muyle, 2014). Determining whether particular components of the genomic selfing syndrome evolve more slowly than that of morphological traits may be difficult because molecular polymorphism and divergence in recently originated selfers may be partly a remnant of their outcrossing ancestry. Comparative analysis of outcrossers and independently derived selfers of contrasting age should provide insights into the relative tempo of morphological and genomic selfing syndrome evolution.

A classic paradigm for studying transitions from outcrossing to selfing is the evolutionary breakdown of the sexual polymorphism heterostyly to homostyly (reviewed in Barrett, 2019, see Fig. 1). Populations with this mating polymorphism most commonly consist of two (distyly) floral morphs that differ reciprocally in stigma and anther position and usually possess heteromorphic self-incompatibility, which limits self- and intra-morph mating (Darwin, 1877; Ganders, 1979; Barrett, 1992). Homostylous individuals are self-compatible and possess stigmas and anthers positioned close to one another within a flower causing autonomous self-pollination and moderate-to-high selfing rates (Piper *et al.*, 1984; Ganders *et al.*, 1985; Yuan *et al.*, 2023). Most mating system transitions in angiosperms evolve gradually, via the loss of self-incompatibility and herkogamy, but in distylous groups, selfing homostyles can arise rapidly through an abrupt rearrangement of sexual organs caused by mutation of genes in the *S*-locus linkage group governing the heterostylous syndrome (reviewed in Kappel *et al.*, 2017).

Primula (Primulaceae) is the most intensively studied heterostylous taxon with the vast majority (92%) of *c.* 400–500 species distylous and the remainder homostylous (Richards, 2003; de Vos *et al.*, 2014). Phylogenetic analyses and ancestral state reconstructions indicate numerous independent transitions from distyly to homostyly, with half of the 38 sections containing homostylous taxa (Mast *et al.*, 2006; de Vos *et al.*, 2014; Zhong *et al.*, 2019). Moreover, intraspecific studies provide compelling evidence that homostyles are derived from distylous morphs (Crosby, 1949; Charlesworth & Charlesworth, 1979; Yuan *et al.*, 2017; Zhou *et al.*, 2017; Shao *et al.*, 2019; Zhang *et al.*, 2021). Our earlier studies of floral traits and molecular evolution among diverse *Primula* species provided evidence for the evolution of morphological (Zhong *et al.*, 2019) and genome-wide selfing syndromes (Wang *et al.*, 2021). Here, we extend this work by focusing on the *P. oreodoxa* complex to investigate time-dependent parallel stages in the development of morphological and genomic syndromes. This complex is comprised of two sister species: *P. oreodoxa* containing distylous and homostylous populations and *P. dumicola* which is exclusively homostylous (Yuan *et al.*, 2017; Zhong *et al.*, 2019).

Our study addressed the following specific questions: (1) Is there evidence for independent origins of homostyly in the *P. oreodoxa* complex? And if so, are homostylous lineages likely to be of different age? Specifically, we evaluate the hypothesis that the exclusively homostylous *P. dumicola* (hereafter 'older homostyles') was derived from a distylous common ancestor earlier than homostyles of *P. oreodoxa* (hereafter 'younger homostyles'). (2) Have both transitions to homostyly resulted in elevated selfing rates compared with distylous ancestors, with older homostyles exhibiting the highest selfing rates. (3) Are these mating-system transitions accompanied by the evolution of morphological and genomic selfing syndromes and, if so, are they at different stages of development in the putatively older vs younger homostyles.

Materials and Methods

Study system

Members of the *Primula oreodoxa* complex (*Primula* subg. *Auganthus* sect. *Obconicolisteri*; Richards, 2003) are herbaceous showy-flowered perennials restricted in distribution to Yunnan and Sichuan Provinces, China (98 to 104°E, 24 to 31°N; Fig. 1). Populations grow along streams and edges of woodlands between 1090 and 3030 m and flower in March–April with fruiting in late May to June. Populations are insect-pollinated, particularly those that are distylous, and visited by bees, flies, and butterflies. Plants are fully self-compatible and the distylous polymorphism is controlled by a single Mendelian *S*-locus with the S-morph dominant to the L-morph, as occurs in most distylous species (Yuan

© 2024 The Authors
New Phytologist © 2024 New Phytologist Foundation

14698137, 0, Downloaded from https://nph.onlinelibrary.wiley.com/doi/10.1111/nph.19522 by Peking University Health, Wiley Online Library on [15/01/2024]. See the Terms and Conditions (https://onlinelibrary.wiley.com/terms-and-conditions) on Wiley Online Library for rules of use; OA articles are governed by the applicable Creative Commons License

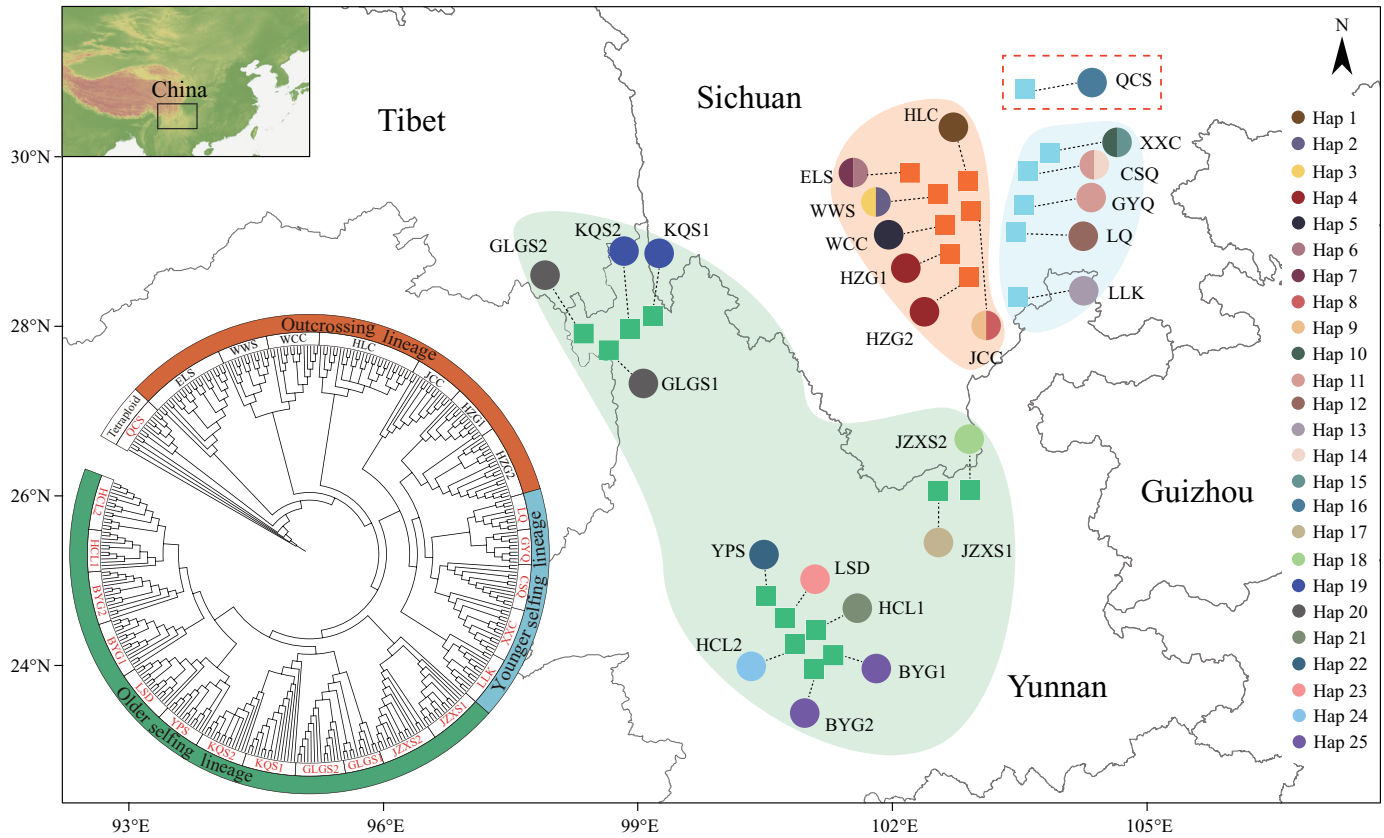

Fig. 1 Geographic distribution of the 25 populations of the *Primula oreodoxa* complex investigated in the study. Each population is distinguished by a letter code and the overall distribution of the three lineages are the color-shaded areas. The squares are sampled populations, with green squares representing homostylous *P. dumicola* populations (older selfing lineage), and the orange and blue squares representing distylous and homostylous *P. oreodoxa* populations (outcrossing lineage and younger selfing lineage), respectively. The colored circles represent the distribution of chloroplast haplotypes within each population. The individual-based NJ tree illustrates the genetic relationships among 378 samples, based on Nei's (1987) unbiased genetic distance calculated from simple sequence repeat (SSR) genotype data.

et al., 2019). Detailed studies of the floral biology, pollinators, and mating systems of distylous and homostylous populations are described in Yuan *et al.* (2017, 2023).

Population sampling, genotyping, and sequencing

We surveyed 13 populations of *P. oreodoxa* Franch. including four distylous populations, three distylous–homostylous populations (homostyles < 5% in frequency), six homostylous populations, and 12 homostylous populations of *P. dumicola* W. W. Sm. & Forrest (Supporting Information Table S1). In each population, we collected leaf tissue from 12 to 32 plants, and this was preserved in either silica gel or liquid nitrogen for subsequent DNA and RNA-seq analysis.

To investigate the phylogeography of the complex, we used 35 samples (1–3 plants per population) to obtain chloroplast genome assemblies and 378 samples (10–29 plants per population) for nuclear simple sequence repeat (SSR) genotyping. Total genomic DNA was extracted from dried leaf tissue using a modified cetyl trimethyl ammonium (CTAB) method (Doyle, 1991). The purified DNA was sheared into *c.* 600 bp fragments to construct a paired-end (PE) library according to the preparation procedures (Illumina, San Diego, CA, USA). We then generated the PE reads (300 bp) using a HiSeq X-Ten sequencer (Illumina). We genotyped 16 microsatellite loci (Table S2) from 378 individuals to assess genetic diversity and population structure of the complex following Zhong *et al.* (2019) and Yuan *et al.* (2018).

We isolated total RNA from 63 samples (2–3 individuals from each population) using an RNAprep Pure Plant Kit (Tiangen Biotechnologies Corporation, Beijing, China). We prepared the cDNA library for transcriptome sequencing using a cDNA Synthesis Kit (Illumina). The cDNA libraries were then sequenced on the Illumina HiSeq 4000 platform (Illumina) to obtain PE reads (2 × 150 bp) of each cDNA. Preprocessing of molecular data for evolutionary analysis is detailed in Methods S1, including the plastome assembly and annotation and SNPs calling from RNA-seq data.

Lineage inference using chloroplast genome data

Phylogenetic inference of haplotypes Using the annotations of chloroplast genomes described in Methods S1, whole plastomes were aligned with MAFFT v.7.487 (Katoh & Standley, 2013), and then haplotypes were retrieved using the grogram DnaSP

© 2024 The Authors
New Phytologist © 2024 New Phytologist Foundation

14698137, 0, Downloaded from https://nph.onlinelibrary.wiley.com/doi/10.1111/nph.19522 by Peking University Health, Wiley Online Library on [15/01/2024]. See the Terms and Conditions (https://onlinelibrary.wiley.com/terms-and-conditions) on Wiley Online Library for rules of use; OA articles are governed by the applicable Creative Commons License

v.6.0 (Rozas *et al.*, 2017). We investigated phylogenetic relationships among haplotypes using maximum likelihood (ML) and Bayesian inference (BI) methods, with *P. densa*, *P. obconica*, and *P. effusa* as outgroups. We used the program ModelTest-NG v.0.1.6 (Darriba *et al.*, 2020) with the Akaike Information Criterion (AIC) to determine the most suitable base substitution model. We performed ML analysis under the program RAxML v.8.2.12 (Stamatakis, 2014) with 1000 pseudoreplicates of rapid bootstrap, and used MrBayes v.3.2.7 (Ronquist & Huelsenbeck, 2003) to infer the optimal tree topology and calculate the posterior probability for the dataset.

Lineage inferences using nuclear genome data

Lineage inference from SSR genotype data To obtain evidence for the hypothesis of independent origins of selfing lineages and to determine relationships among lineages, we investigated patterns of differentiation among surveyed populations with different floral morph structures by the following methods. First, we constructed a consensus neighbor-joining (NJ) tree based on Nei's (1987) unbiased genetic distance matrix with random input order of 1000 bootstraps in Phylip v.3.63 (Felsenstein, 2005). Then, we calculated a Euclidean distance matrix of all samples and created a visual representation of genetic relationships among samples using principal coordinate analysis (PCA) in the program GenAlEx v.6.501 (Peakall & Smouse, 2006). Finally, we inferred the genetic structure of populations in InStruct 1.0 (Gao *et al.*, 2007), which uses a model similar to Structure (Pritchard *et al.*, 2000), but incorporates inbreeding. A total of 20 independent simulations were run for each K (2–15), which contained 5×10^5 burn-in steps followed by 5×10^5 MCMC steps. The optimal K value was determined according to the program Clumpak 1.0 (Kopelman *et al.*, 2015).

Lineage inference from SNP data We also performed a Bayesian clustering analysis and PCA based on SNPs retrieved from the RNA-seq data. For these analyses, we retained 4-fold synonymous SNPs with minor allele frequencies (MAF) < 0.05 removed. We used fastSTRUCTURE (Raj *et al.*, 2014) to investigate population structure, with the five independent replicates for each number of clusters (K) being set from 2 to 15. The script chooseK.py was used to determine the optimal K value. Based on the same dataset, we performed a PCA by Plink v.1.90 (Purcell *et al.*, 2007) and constructed a ML tree by using RAxML v.8.2.12 (Stamatakis, 2014) with *P. obconica* (SRAID: SRR866502) and *P. forbesii* (SRAID: SRR3355030) as outgroups.

Tests of lineage differentiation history by ABC modeling - Based on our inferences on lineage clustering described previously, we identified three lineages: the distylous lineage of *P. oreodoxa* (D-Po), the homostylous lineage of *P. oreodoxa* (H-Po), and the homostylous lineage of *P. dumicola* (H-Pd). Four alternative models of population history were summarized (Fig. S1) and simulated under an approximate Bayesian computation (ABC) procedure (Beaumont *et al.*, 2002) using the program DIYABC v.2.1.0 (Cornuet *et al.*, 2008). We repeated 4×10^5 simulations to obtain a reference table for each model. To compare the posteriori probabilities of the four models, we selected the 1×10^5 (20%) simulated datasets for logistic regression and calculated the posteriori probability and 95% confidence intervals (CI). After choosing the best model, we estimated parameter posterior distributions by using 1×10^5 (20%) simulated datasets.

Selfing rates

We estimated population-level selfing rates using the program RMES (David *et al.*, 2007) under two different scenarios: two-locus heterozygosity disequilibrium (g2, correlation selfing rate s (g2)), and the maximum log-likelihood of multiple heterozygotes (s(ML)). We conducted 1×10^4 iterations of randomly reassorting single-locus heterozygosity among individuals, with a maximum of 15 generations of selfing and a precision of 1×10^{-5} log-likelihood in each case.

Quantifying the genomic selfing syndrome

Nucleotide diversity and polymorphism To assess variation in genetic diversity among the three lineages, we estimated population statistics of pairwise nucleotide diversity (π), Watterson's theta (θ_W), and Tajima's D for both synonymous and nonsynonymous sites. We then conducted an MK test (McDonald & Kreitman, 1991) to determine whether the ratio of nonsynonymous to synonymous polymorphisms ($P_N : P_S$) of each lineage was differentiated from the ratio of nonsynonymous to synonymous divergence ($D_N : D_S$) of the outgroup species (*P. densa* and *P. obconica* for chloroplast and nuclear genomes, respectively). We summarized the MK results using the NI index defined as $(P_N : D_N)/(P_S : D_S)$ (Rand & Kann, 1996). All analyses were separately conducted for the datasets of both coding sequences (CDS) of nuclear genes and chloroplast genes.

Mutation loads and selection efficacy To compare the genetic load of the three lineages, we annotated and classified the effects of nonsynonymous and synonymous SNP variants on protein coding sequences using the program SIFT 4G (Vaser *et al.*, 2016). Nonsynonymous SNPs were subsequently classified as either deleterious (score ≤ 0.05) or tolerated (score > 0.05) based on the SIFT score. We then assessed the proportion of recessive ($\delta N_{homo}/\delta S$) and additive ($\delta N_{hete}/\delta S$) genetic loads by using the weighted amount of homozygous and heterozygous deleterious mutations with the number of synonymous variants (δS), respectively.

To quantify variation of selection efficacy among lineages, we inferred the distribution of fitness effects (DFE) and the proportion of adaptive substitutions (α) for new nonsynonymous mutations using DFE-α v.2.16 (Schneider *et al.*, 2011). First, we generated the unfolded site frequency spectra (SFS) for each lineage based on synonymous and nonsynonymous loci with *P. obconica* and *P. forbesii* as outgroups. Then, we inferred the DFE under a two-epoch model considering the potential change of population size especially for homostylous lineages. The DFE for

© 2024 The Authors
New Phytologist © 2024 New Phytologist Foundation

14698137, 0, Downloaded from https://nph.onlinelibrary.wiley.com/doi/10.1111/nph.19522 by Peking University Health, Wiley Online Library on [15/01/2024]. See the Terms and Conditions (https://onlinelibrary.wiley.com/terms-and-conditions) on Wiley Online Library for rules of use; OA articles are governed by the applicable Creative Commons License

each lineage was then summarized in four bins representing increased purifying selection (0–1, 1–10, 10–100, and >100). The proportion of adaptive (ω_α) and nonadaptive (ω_d) substitution for each lineage among all nonsynonymous substitutions was inferred from the unfolded SFS. The 95% confidence intervals (CI) were generated by using 200 bootstrap replicates randomly sampled from the original SFS.

Quantifying the morphological selfing syndrome

Measurement of morphological traits To investigate the morphological selfing syndrome following shifts in mating system, we obtained a random sample of 866 flowers (distylous *P. oreodoxa*: $n = 336$ flowers, $n = 6$ populations; homostylous *P. oreodoxa*: $n = 147$ flowers, $n = 5$ populations; homostylous *P. dumicola*: $n = 383$ flowers, $n = 12$ populations) from 23 populations of the *P. oreodoxa* complex (Table S1) with 1–3 flowers from each plant. We also sampled *c.* 30 unopened flowers from on average 20 plants in each population for pollen and ovule counts. Flowers were classified according to floral morph (L-morph, S-morph, and H-morph) based on the positions of their sexual organs before being preserved in 75% ethanol for subsequent measurement. We measured 22 floral traits, see Methods S1, to quantify morphological difference among lineages.

Statistical analyses We estimated the distribution of stigma and anther height by using a ML-based method (Zhou *et al.*, 2017) and classified flowers into three floral morphs. Because our preliminary analysis revealed high correlations among some morphological traits (Fig. S2), and to avoid bias caused by multiple ANOVAs, we used multivariate analyses of variance (MANOVAs) followed by ANOVAs to determine lineage variation in phenotypic traits. We analyzed all of the measured traits in MANOVAs and repeated the analysis by grouping the floral traits in two different categories (Table S3): floral display (e.g. flower size measurements) and floral allocation (e.g. pollen and ovule investment and nectar production) traits. Response variables were log-transformed with the function $y = \log(x + 1)$ to improve the normality of residuals and homoscedasticity. We used Wilks' lambda (λ) to evaluate significance in MANOVA models and then protected ANOVAs were carried out for each variable to examine the effects of lineage, population, and floral morph.

Additionally, we also performed PCA to provide a graphical description of how each trait contributed to observed differences among lineages. We calculated PCAs as independent linear combinations of the standardized original variables with the same transformation as in the MANOVAs. For the three distylous–homostylous populations of *P. oreodoxa* (Table S1), we excluded the morphological data of homostyles and treated the populations as distylous in the above analysis because of the low frequency (< 5%) of homostyles in these populations. Three traits (stigma and anther height and pollen size) were excluded from the MANOVA and PCAs as the traits involve intrinsic difference between distylous floral morphs. We conducted all analyses in R v.4.1 (R Core Team, 2021).

Results

Lineage differentiation within the *P. oreodoxa* complex

We assembled 35 complete plastid genomes for the *P. oreodoxa* complex (Table S4). The whole plastome dataset exhibited considerable polymorphism and comprised a total of 25 haplotypes (Hap1–Hap25). The geographical distribution of haplotypes is illustrated in Fig. 1, which shows three distinct groups that are mostly allopatric. All *P. dumicola* populations contained a single haplotype and three distylous and two homostylous population of *P. oreodoxa* contained two haplotypes.

The haplotype trees obtained from ML and Bayesian methods were largely congruent in topology (Fig. 2a), and the *P. oreodoxa* complex was strongly supported as monophyletic (ML bootstrap value 100%; Bayesian posterior 1.00), with all haplotypes (except Hap16, see below) clustered into three lineages with strong nodal supports. A distinct lineage included all samples (Hap17–Hap25) of homostylous *P. dumicola*, and we infer that this represents an early independent origin of homostyly (hereafter referred to as 'older selfing lineage' or H-Pd). The remaining haplotypes were all recovered from *P. oreodoxa*, with haplotypes (Hap1–Hap9) from distylous populations forming an exclusively distylous lineage (hereafter referred to as 'outcrossing lineage' or D-Po), and the remaining haplotypes (Hap10–Hap15) forming a more recently derived homostylous lineage (hereafter referred to as 'younger selfing lineage' or H-Po; Fig. 2a). Consistent with an earlier study (Zhong *et al.*, 2019), the haplotype (Hap16) recovered from the only known tetraploid ($2n = 48$) population (QCS) of homostylous *P. oreodoxa* was located at the base of the complex and may represent another independent origin of homostyly.

Structure analysis of SSR genotypes and synonymous SNPs both recovered a local peak of ΔK values at $K = 2$, which clearly divided the complex into a *P. dumicola* lineage and a *P. oreodoxa* lineage (Fig. 2b,c). Although populations of homostylous *P. oreodoxa* formed a cluster (Fig. 2b,c), they were not clearly separated from the remaining distylous populations when increasing the cluster (K) number. The genetic similarity between the more recently derived homostylous lineage (younger selfing lineage) and its ancestral outcrossing distylous lineage was also evident by two-dimensional PCA of SSR phenotypes (Fig. 2d) and high-density SNPs (Fig. 2e). Samples from younger selfing and distylous populations largely overlapped, although all were clearly separated from samples of the older *P. dumicola* selfing lineage (Fig. 2d,e).

In the DIYABC analysis, four alternative models of evolutionary differentiation were analyzed (Table S5) and the posterior probabilities for evolutionary model 2 was 0.954 (95% CI: 0.921–0.987), much higher than for the other scenarios (model 1: 0.005, model 3: 0.021, and model 4: 0.020). Model 2 (Fig. 3a) depicted an evolutionary history in which the older selfing lineage diverged first from the ancestor of the distylous *P. oreodoxa* lineage followed by the younger selfing lineage. The estimated posterior distribution of parameters for best model are presented in Table S5.

© 2024 The Authors
New Phytologist © 2024 New Phytologist Foundation

14698137, 0, Downloaded from https://nph.onlinelibrary.wiley.com/doi/10.1111/nph.19522 by Peking University Health, Wiley Online Library on [15/01/2024]. See the Terms and Conditions (https://onlinelibrary.wiley.com/terms-and-conditions) on Wiley Online Library for rules of use; OA articles are governed by the applicable Creative Commons License

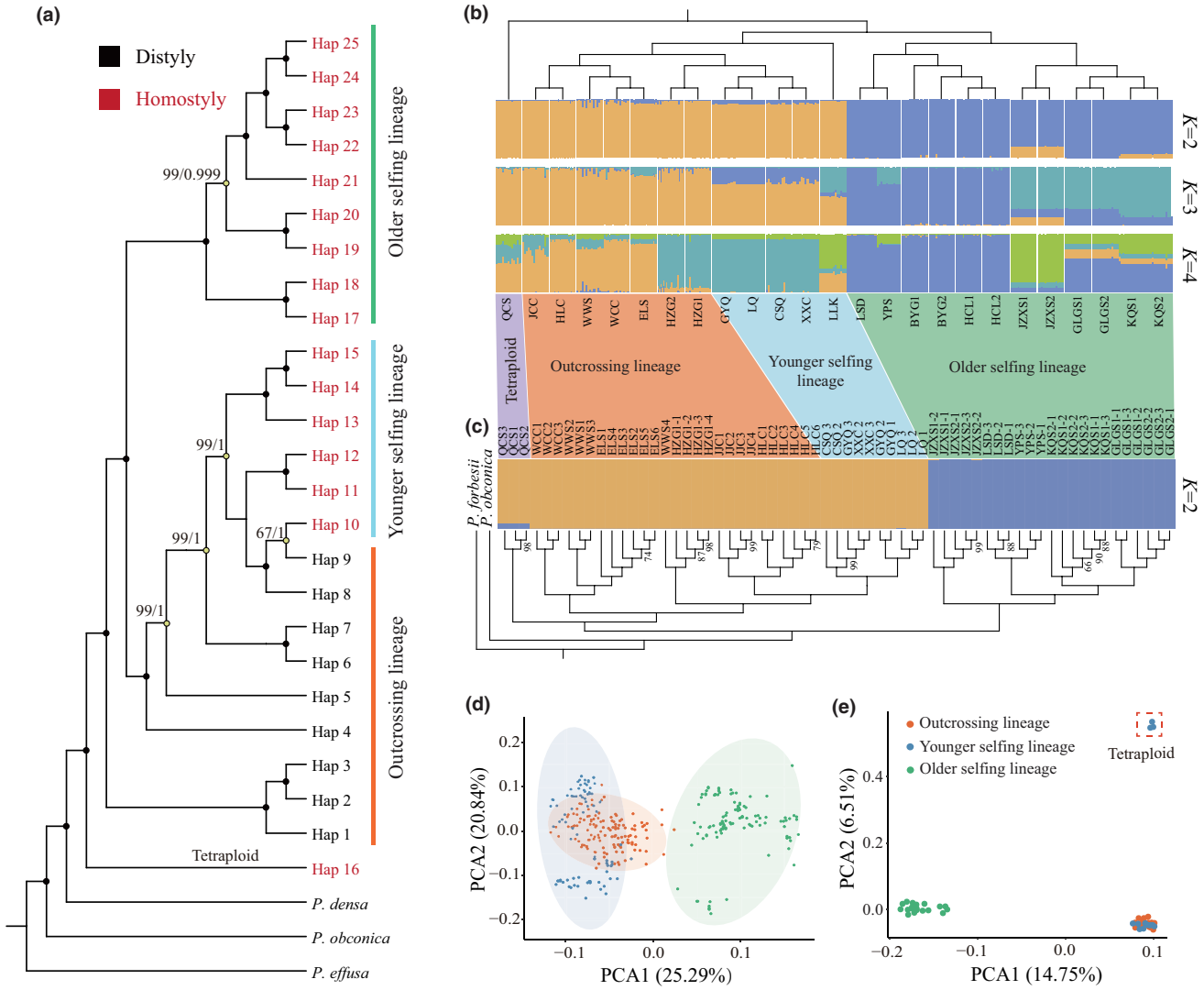

Fig. 2 Haplotype phylogenetic tree and population genetic structure of population samples from the *Primula oreodoxa* complex. (a) Haplotype phylogenetic framework constructed from data from the chloroplast genome. ML bootstrap values below 100 and Bayesian posterior probabilities below 1 are indicated at nodes. (b, c) Population cluster analysis and a maximum likelihood (ML) phylogenetic tree based on simple sequence repeat (SSR) genotypes and synonymous SNPs datasets, respectively. ML bootstrap values below 100 are indicated at nodes. (d, e) Principal component analysis (PCA) of the SSR genotypes of 378 individuals and synonymous SNPs of 63 samples, respectively. Red, blue, and green dots represent samples from outcrossing, younger selfing, and older selfing lineages, respectively.

Selfing rates

Selfing rates varied among the three lineages; as expected, the distylous lineage had the lowest level of selfing (s(g2) = 0.203, s (ML) = 0.127), whereas much higher levels of selfing occurred in both the younger (s(g2) = 0.776, s(ML) = 0.718) and older selfing lineages (s(g2) = 0.896, s(ML) = 0.906) (Fig. 3b). Population differentiation measured using F_{st} gave values of 0.103, 0.127, and 0.144 for the distylous, the younger selfing and the older selfing lineages, respectively.

Genomic selfing syndrome

Patterns of genetic diversity were similar between the nuclear and chloroplast genomes of samples of the *P. oreodoxa* complex (Table 1). Compared with the outcrossing distylous lineage, levels of polymorphism for both younger and older selfing lineages were significantly reduced. In the nuclear genome, the ratio of nonsynonymous to synonymous nucleotide diversity ($\pi_N : \pi_S$ and $\theta_N : \theta_S$) was higher in the older selfing lineage ($\pi_N : \pi_S = 0.248$, $\theta_N : \theta_S = 0.256$) than in the outcrossing lineage (0.199, 0.208), whereas the younger selfing lineage (0.237, 0.249) was slightly lower than that of the older selfing lineage, a pattern consistent with the results of MK tests described below. For the chloroplast coding regions, the $\pi_N : \pi_S$ and $\theta_N : \theta_S$ of the older selfing lineage (0.537, 0.563) were higher than that of the outcrossing lineage (0.333, 0.334) or the younger selfing lineage (0.218, 0.261). Values for Tajima's D of younger and older selfing lineages were higher than that of the outcrossing lineages for both nuclear and chloroplast genomes.

© 2024 The Authors
New Phytologist © 2024 New Phytologist Foundation

14698137, 0, Downloaded from https://nph.onlinelibrary.wiley.com/doi/10.1111/nph.19522 by Peking University Health, Wiley Online Library on [15/01/2024]. See the Terms and Conditions (https://onlinelibrary.wiley.com/terms-and-conditions) on Wiley Online Library for rules of use; OA articles are governed by the applicable Creative Commons License

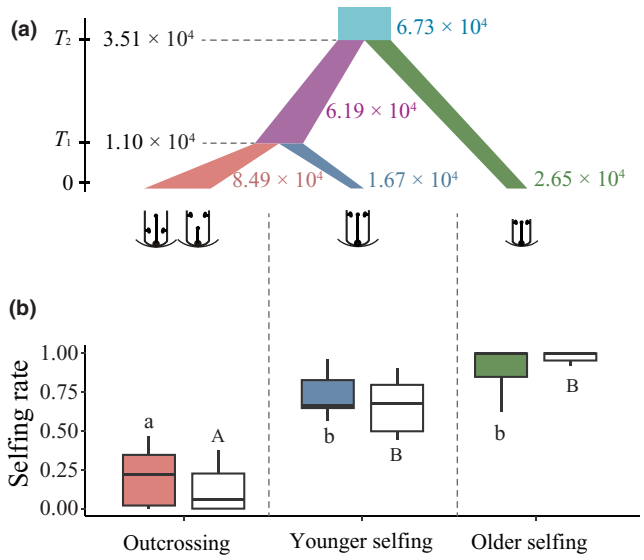

Fig. 3 Diagram of lineage differentiation history and estimated selfing rates of each lineage in the *Primula oreodoxa* complex. (a) Diagram portraying the best-fitting model of the history of evolutionary divergence and differentiation for the three lineages in the *P. oreodoxa* complex. T_1 and T_2 represent the time of origin of young and old selfing lineages in generations before present, respectively. Colored numbers indicate the effective population size in the corresponding lineages. (b) Closed and opened boxplot indicate selfing rates calculated by *s*(g2) and *s*(ML), respectively. Significant differences ($P < 0.01$) are indicated by different letters. Boxplot legend: upper and lower horizontal lines of box indicate 75th and 25th percentile, respectively; within box line and vertical line indicated the median and minimum–maximum value, respectively.

The NI value of the outcrossing lineage was not significantly different from one for both datasets (nuclear genome: NI = 1.025, $P = 0.172$; chloroplast genome: NI = 0.965, $P = 0.825$; Fig. 4a,b) consistent with the null expectation of equal ratios of polymorphism and divergence. By contrast, both younger and older selfing lineages exhibited significant deviations from neutrality, with higher NI values for nuclear loci (Fig. 4a) and therefore evidence for the accumulation of slightly deleterious mutations. We also found that the effect of selfing on NI values of the chloroplast genomes depended on whether the selfing lineage was derived earlier or more recently. The NI value of the younger selfing lineage (NI = 0.786, $P = 0.587$) was similar to the outcrossing lineage (NI = 0.965, $P = 0.825$) with both close to 1, whereas it was significantly higher (NI = 1.736, $P = 0.009$) for the older selfing lineage (Fig. 4b).

The outcrossing lineage had significantly fewer deleterious heterozygous and homozygous nonsynonymous mutations (Fig. 4c,d). A higher recessive load was observed in the older than the younger selfing lineage (Fig. 4c), whereas there was no significant difference in additive loads between the two selfing lineages (Fig. 4d).

Based on the unfolded site frequency spectra (SFS) (Fig. S3), our DFE analysis indicated that the outcrossing lineage had accumulated relatively fewer effectively neutral nonsynonymous mutations with 14.84% falling into the category ($0 < N_e s < 1$) (Fig. 4e). By contrast, a significantly higher proportion of sites were classified as having effectively neutral mutations in both selfing lineages (25.37%—older selfing lineage; 21.59%—younger selfing lineage). Notably, strongly deleterious mutations ($N_e s > 100$) were prevalent in both the younger (60.35%) and older selfing lineage (66.64%).

The proportion of adaptive substitutions for each selfing lineage was significantly lower than that of the outcrossing lineage (Table 2). The estimate of α fixed by positive selection between the outcrossing lineage and the outgroup was 64%, whereas no adaptive substitutions were found for each of the selfing lineages because α was either negative or close to zero (Table 2). The negative estimates of α probably reflect the downward bias introduced by the presence of weakly deleterious variants in selfing lineages. By partitioning nonsynonymous substitutions into adaptive (ω_α) and nonadaptive (ω_d) proportions, lower ω_α and higher ω_d values were obtained in both selfing lineages compared with the outcrossing lineage (Table 2).

Table 1 Summary of chloroplast and nuclear genome data for the three identified lineages (outcrossing, younger selfing and older selfing) of the *Primula oreodoxa* complex.

Lineage	*n*	Site class	N_{sites}	*S*	π (10^{-2})	θ_W (10^{-2})	$\pi_N : \pi_S$	$\theta_N : \theta_S$	Tajima's *D*
(a) Nuclear genome									
Outcrossing lineage (D-Po)	13	Synonymous	895 491	21 081	0.492	0.654	0.199	0.208	−0.437
		Nonsynonymous	4073 447	19 937	0.098	0.136			
Younger selfing lineage (H-Po)	13	Synonymous	738 080	6074	0.207	0.229	0.237	0.249	0.924
		Nonsynonymous	3419 678	7009	0.049	0.057			
Older selfing lineage (H-Pd)	13	Synonymous	758 124	4354	0.129	0.160	0.248	0.256	1.128
		Nonsynonymous	3495 143	5130	0.032	0.041			
(b) Chloroplast genome									
Outcrossing lineage (D-Po)	12	Synonymous	15 218	137	0.321	0.290	0.333	0.334	0.282
		Nonsynonymous	50 452	152	0.107	0.097			
Younger selfing lineage (H-Po)	7	Synonymous	15 214	17	0.055	0.046	0.218	0.261	0.536
		Nonsynonymous	50 438	15	0.012	0.012			
Older selfing lineage (H-Pd)	14	Synonymous	15 207	43	0.107	0.087	0.537	0.563	0.709
		Nonsynonymous	50 415	81	0.057	0.049			

Nucleotide diversity (π), Watterson's theta (θ_W) and test for neutrality (Tajima's *D* based on π and θ_W) for each lineage are given. *n*, sample size; N_{sites}, number of sites; *S*, number of polymorphisms.

© 2024 The Authors
New Phytologist © 2024 New Phytologist Foundation

14698137, 0, Downloaded from https://nph.onlinelibrary.wiley.com/doi/10.1111/nph.19522 by Peking University Health, Wiley Online Library on [15/01/2024]. See the Terms and Conditions (https://onlinelibrary.wiley.com/terms-and-conditions) on Wiley Online Library for rules of use; OA articles are governed by the applicable Creative Commons License

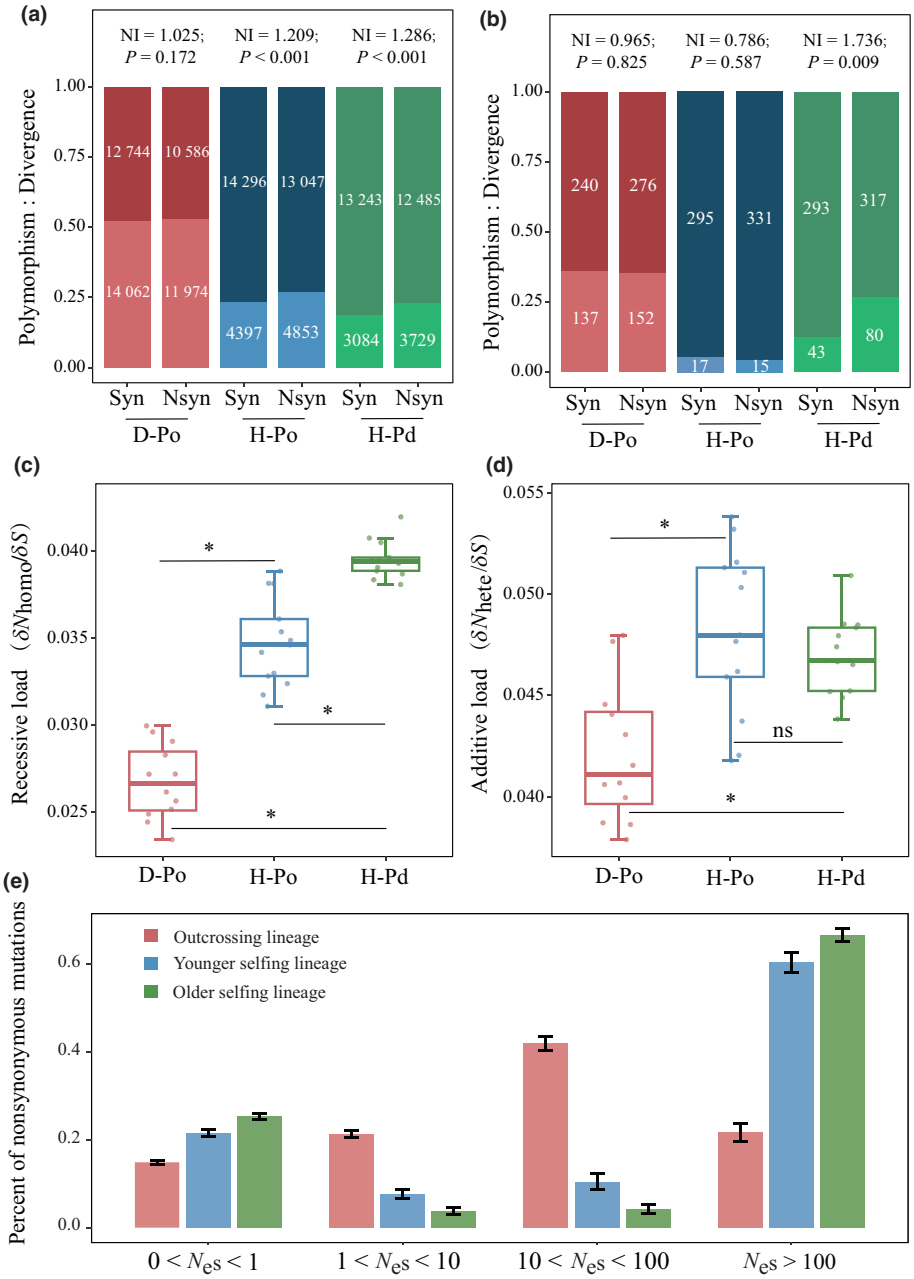

Fig. 4 Genetic load and selection efficacy comparisons among outcrossing (D-Po), younger selfing (H-Po), and older selfing (H-Pd) lineages of the *Primula oreodoxa* complex. MK tests were performed on three lineages using (a) nuclear and (b) chloroplast genome data, with *P. obconica* and *P. densa* as outgroup, respectively. Stacked bars indicate the proportion of polymorphism (lower part) and divergence (upper part) in synonymous (P_S and D_S) and nonsynonymous (P_N and D_N) sites, respectively. NI—the neutrality index calculated as $(P_N : D_N)/(P_S : D_S)$. (c, d) represent the recessive and additive genetic load, respectively. Significant differences indicated above plot by ns, $P > 0.05$; *, $P < 0.001$. Boxplot legend: upper and lower horizontal lines indicated the 75th and 25th percentiles, respectively. The central line and the whiskers indicated the median and minimum–maximum values. Circle indicated the data point of each individual. (e) The distribution of fitness effects (DFE) of new nonsynonymous mutations fall into different $N_e s$ categories for the three lineages. $N_e s$ is the product of effective population size (N_e) and the selection coefficient (s). Thirteen individuals for each lineage were used to generate the DFEs. Error bars for each $N_e s$ category represent 95% confidence intervals from 200 bootstrap replicates generated by resampling over loci. The differences were all significant ($P < 0.001$) among the three lineages within each $N_e s$ category.

Morphological selfing syndrome

As expected, the heights of stigmas and anthers in the L- and S-morphs exhibited clear bimodal distribution, whereas sexual organs had a unimodal distribution in both homostylous lineages (Fig. S4). In the distylous lineage, there was almost perfect spatial matching between corresponding sexual organs of the floral morphs and almost no overlap between incompatible stigmas and anthers (Fig. S4). Thus, herkogamy was well-developed in the distylous morphs but either absent or weakly developed in the selfing homostylous lineages, with approach and reverse herkogamy evident in both homostylous lineages (Fig. S4).

The three lineages differed in floral morphological traits in both the combined (MANOVA, Wilks' $\lambda = 0.317$, $F_{20,67} = 7.192$, $P < 0.001$) or separate analyses based on the two floral categories (floral display: Wilks' $\lambda = 0.043$, $F_{24,366} = 57.686$, $P < 0.001$; floral allocation: Wilks' $\lambda = 0.606$, $F_{8,94} = 7.621$, $P < 0.001$). The outcrossing lineage had a greater floral display traits (e.g. floral size and color), more investment in male reproductive function (e.g. pollen number and P : O ratio), and pollinator rewards (e.g. sugar volume and concentration) (ANOVAs, Fig. 5; Table S3) than the two selfing lineages. The younger selfing lineage was generally intermediate in trait values and differed significantly from the other lineages in most morphological traits (Fig. 5; Table S3), but with some exceptions. For example, values for ovule number (Fig. 5o) and petal color (RGB value) (Fig. 5s) of the younger selfing lineage overlapped with the outcrossing lineage, whereas P : O ratios (Fig. 5p) and corolla mouth

© 2024 The Authors
New Phytologist © 2024 New Phytologist Foundation

14698137, 0, Downloaded from https://nph.onlinelibrary.wiley.com/doi/10.1111/nph.19522 by Peking University Health, Wiley Online Library on [15/01/2024]. See the Terms and Conditions (https://onlinelibrary.wiley.com/terms-and-conditions) on Wiley Online Library for rules of use; OA articles are governed by the applicable Creative Commons License

14698137, 0, Downloaded from https://nph.onlinelibrary.wiley.com/doi/10.1111/nph.19522 by Peking University Health, Wiley Online Library on [15/01/2024]. See the Terms and Conditions (https://onlinelibrary.wiley.com/terms-and-conditions) on Wiley Online Library for rules of use; OA articles are governed by the applicable Creative Commons License

Table 2 Parameters of the fitness distribution of nonsynonymous mutations (β, mean S), rate of adaptive evolution (α), adaptive (ω_α) and non-adaptive proportion (ω_d) of $d_N : d_S$ for each studied lineage (outcrossing, younger selfing and older selfing) of the *Primula oreodoxa* complex estimated with the method of DFE.

	Outcrossing lineage (D-Po)	Younger selfing lineage (H-Po)	Older selfing lineage (H-Pd)
β (CI)	0.392 (0.359, 0.425)	0.132 (0.119, 0.145)	0.060 (0.047, 0.073)
Mean S (CI)	68.319 (64.250, 72.388)	1.01×10^5 (5.14×10^4, 1.50×10^5)	2.77×10^{10} (2.30×10^{10}, 3.24×10^{10})
α (CI)	0.638 (0.603, 0.673)	−0.058 (−0.096, −0.020)	−0.224 (−0.240, −0.209)
ω_α (CI)	0.223 (0.209, 0.238)	−0.010 (−0.014, −0.007)	−0.045 (−0.065, −0.023)
ω_d (CI)	0.125 (0.104, 0.146)	0.199 (0.177, 0.221)	0.243 (0.222, 0.265)

β, the shape parameter of the gamma distribution assumed for the estimations of S.

width (Fig. 5k) were similar between the two selfing lineages. As expected, pollen grains exhibited size dimorphism between the L- and S-morphs within the distylous lineage (Fig. 5t). The mean pollen size of younger homostyles (21.36 ± 2.84) was similar to the S-morph of the distylous lineage, whereas the pollen size of older homostyles (18.13 ± 2.00) was significantly reduced compared with both the S-morph ($F = 612.3$, $P < 0.001$) and the younger homostyles ($F = 1077$, $P < 0.001$) (Fig. 5t).

The morphological transitions from distyly in the younger and old homostylous lineages were also confirmed by PCA (Fig. 6). The first principal component (PC1 = 70.2%) effectively distinguished the outcrossing, younger selfing, and older selfing lineages (Fig. 6a) with comparable contributions from each trait (Fig. 6b). The second component (PC2 = 6.3%) explained a much smaller proportion of the overall variance among lineages (Fig. 6c).

Discussion

Our phylogenomic and population genetic analyses of the *P. oreodoxa* complex revealed that the breakdown of distyly to homostyly has occurred on several occasions resulting in at least two independent selfing lineages. These involve an older derived lineage comprised of a geographically isolated cluster of selfing populations and a relatively younger lineage of selfing populations adjacent to distylous populations, although still allopatric in distribution (Figs 1 and 2). As predicted, the older selfing lineage exhibited more fully developed genomic (Fig. 4; Table 1) and morphological (Figs 5 and 6) selfing syndromes, consistent with a longer evolutionary history of selfing. Nevertheless, the younger selfing lineage also showed parallel changes in morphological and genomic features, although these signatures of selfing were often less well-developed, as expected if the transition to selfing was more recent. Indeed, from the perspective of genome evolution, although not necessarily morphological evolution, both transitions can be considered relatively recent.

An unexpected finding was the substantial changes in the genome of the younger selfing lineage compared with distylous populations (Fig. 4; Table 1). This result contrasts with the theoretical prediction that significant genomic changes resulting from relaxed selection and genetic drift require substantial time periods compared with the more rapid adaptive changes expected for many morphological traits (Glémin & Galtier, 2012; Ness *et al.*, 2012; Slotte *et al.*, 2013; Cutter, 2019). Below, we consider this issue by examining the reproductive, ecological, and population genetic processes influencing the relative tempo of genomic and morphological changes in selfing syndromes.

Evolution of genomic selfing syndromes

We detected an elevated ratio of nonsynonymous to synonymous polymorphism ($\pi_N : \pi_S$) in both the older and younger selfing lineages of *P. oreodoxa* in comparison with the outcrossing lineage (Table 1). The accumulation of deleterious mutations in selfing lineages was supported by a significant increase in the proportion of effectively neutral nonsynonymous mutations (Fig. 4e), a pattern evident in the results from MK tests (Fig. 4a,b). These results are in accord with several previous studies of predominantly selfing species (Slotte *et al.*, 2013; Arunkumar *et al.*, 2015; Chen *et al.*, 2017; Wang *et al.*, 2021); but the significant genomic decay that we detected in the younger selfing lineage was unexpected. Values of $\pi_N : \pi_S$ ($\theta_N : \theta_S$) and the proportion of nonsynonymous mutations substantially increased from those measured in the outcrossing lineage (Fig. 4a,b). This finding is puzzling when the mating systems of populations that we investigated are considered.

Persistently high selfing rates (e.g. $s > 90\%$) is generally considered a key requirement for the gradual evolution of the genomic selfing syndrome, although a small degree of outcrossing may be sufficient to purge deleterious mutations and limit populations from being trapped in the evolutionary 'dead end' of genomic decay (Barrett *et al.*, 2014; Kamran-Disfani & Agrawal, 2014; Laenen *et al.*, 2018; Yi *et al.*, 2022). In our study, selfing rates in homostylous populations ranged from 0.718 to 0.776 and from 0.896 to 0.906 for the younger and older selfing lineages, respectively (Fig. 3b), but moderate amounts of outcrossing were evident in populations of both lineages.

We note that our method for estimating selfing rates from molecular data using the program RMES (David *et al.*, 2007) was indirect and possibly less precise than methods using family-based data (e.g. Wang *et al.*, 2012). However, similar selfing estimates have also been reported using this latter method for homostylous populations of the younger selfing lineage of *P. oreodoxa* (LWP = 0.71 and XXC = 0.63; Yuan *et al.*, 2023). This finding suggests that mixed mating rather than predominant selfing is characteristic of homostylous populations, perhaps because of weakly developed herkogamy in *P. oreodoxa* homostyles (Yuan *et al.*, 2017, 2023), a pattern also reported in other homostylous

© 2024 The Authors
New Phytologist © 2024 New Phytologist Foundation

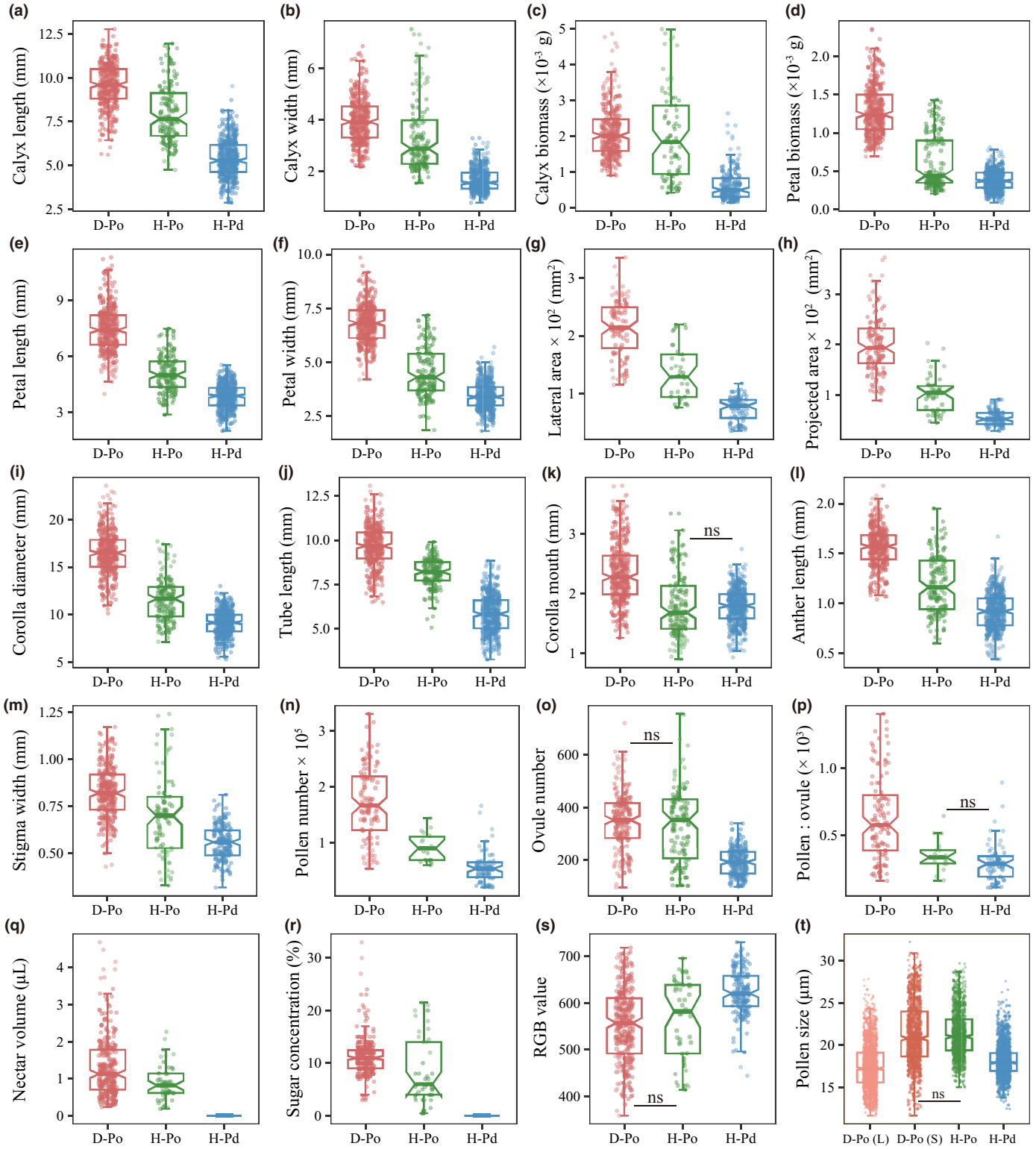

Fig. 5 Box plots illustrating the measurements of floral traits in each studied lineage of the *Primula oreodoxa* complex. (a) calyx length; (b) calyx width; (c) calyx biomass; (d) petal biomass; (e) petal length; (f) petal width; (g) lateral area of flower; (h) projected area of flower; (i) corolla diameter; (j) corolla tube length; (k) corolla mouth; (l) anther length; (m) stigma width; (n) pollen number; (o) ovule number; (p) pollen: ovule ratio; (q) nectar volume; (r) sugar concentration cumulative value; (s) petal color RGB cumulative value; (t) pollen size. D-Po, outcrossing lineage; H-Po, younger selfing lineage; H-Pd, older selfing lineage; L, long-styled morph; S, short-styled morph. The differences were all significant ($P < 0.01$) among the three lineages except the pairs marked with 'ns'. Boxplot legend: upper and lower horizontal lines indicate 75th and 25th percentile, respectively. The central line and the whiskers indicated the median and minimum–maximum values. Circle indicated the data point of each sample.

© 2024 The Authors
New Phytologist © 2024 New Phytologist Foundation

14698137, 0, Downloaded from https://nph.onlinelibrary.wiley.com/doi/10.1111/nph.19522 by Peking University Health, Wiley Online Library on [15/01/2024]. See the Terms and Conditions (https://onlinelibrary.wiley.com/terms-and-conditions) on Wiley Online Library for rules of use; OA articles are governed by the applicable Creative Commons License

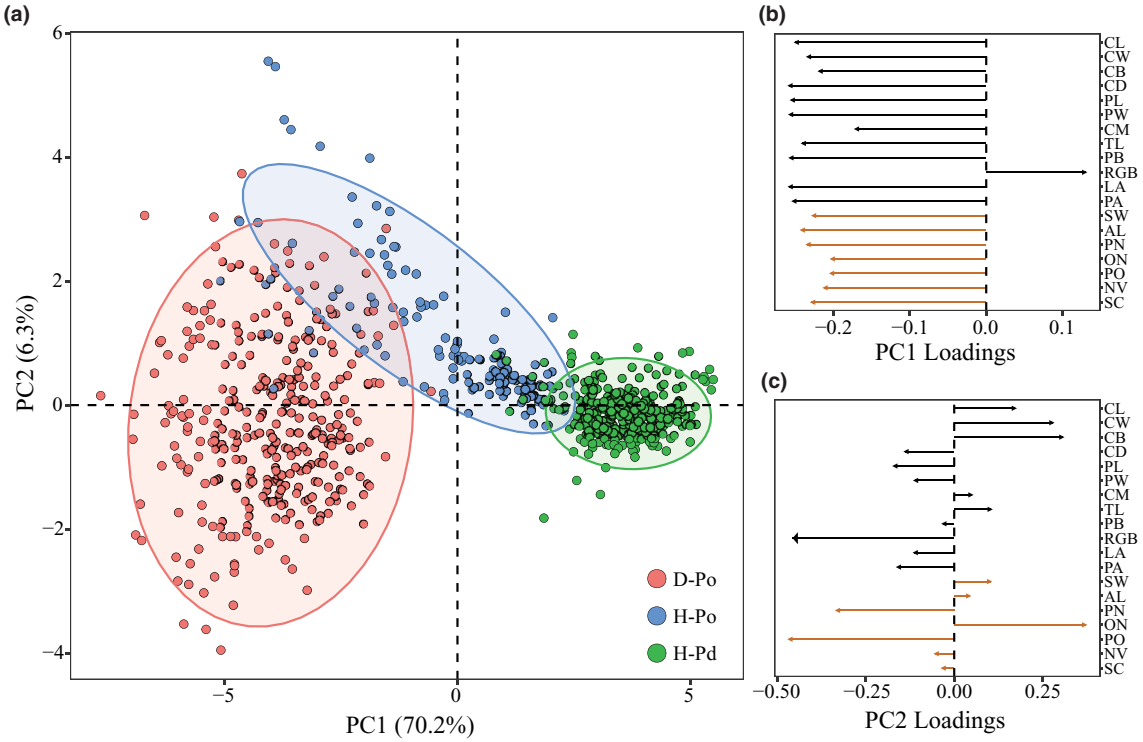

Fig. 6 Principal components analysis (PCA) of 19 phenotypic traits in the *Primula oreodoxa* complex. (a) The PCA results display individual data points, and the proportion of the variance explained is 70.2% and 6.3% for PC1 and PC2, respectively. (b, c) The decomposition of PC1 and PC2, respectively. Black and orange arrows represent the categories of floral-display and floral-allocation traits, respectively. Trait codes are identified in Supporting Information Methods S1.

Primula species (de Vos *et al.*, 2018). If this inference of a history of mixed mating is correct, the apparent emergence of the genomic selfing syndrome in the younger lineage of *P. oreodoxa* is somewhat unexpected.

A second key factor influencing the evolution of the genomic selfing syndrome is the effective population size (N_e), which can directly influence rates of molecular evolution (Ohta, 1992). The reduction of N_e in selfers should magnify the role of genetic drift relative to selection resulting in a higher proportion of new mutations behaving almost neutrally (Akashi *et al.*, 2012). When all else is equal, complete self-fertilization ($F_{IS} = 1$) should lead to a 2-fold reduction of N_e compared with random mating ($F_{IS} = 0$) since $N_e = N/(1 + F_{IS})$. However, since some degree of outcrossing appears to be a feature of *P. oreodoxa* homostyles, reductions in N_e owing to the mating system alone are likely to be less severe and therefore demographic factors may play a more important role. Specifically, the rapid origin of homostyles in *Primula* by single-gene loss of function mutations of CYP^T initially (Huu *et al.*, 2016; Kappel *et al.*, 2017; Mora-Carrera *et al.*, 2023) likely involves severe bottlenecks and could play a significant role in reducing N_e. Such effects on N_e would be further magnified by colonizing episodes because of the capacity of homostyles to found colonies through autonomous self-pollination by single individuals. The demographic history of homostyles, involving genetic bottlenecks in their origin in concert with lineage expansion through colonization, may help to explain why a strong signature of the genomic selfing syndrome was evident in the younger selfing lineage of *P. oreodoxa* complex despite moderate outcrossing. Our inferences on genetic load, however, should be treated cautiously because of the possible nonequilibrium demographic history of the populations we investigated (Brandvain & Wright, 2016).

In contrast to the nuclear genomic effects of contrasting mating systems in the *P. oreodoxa* complex, the accumulation of deleterious mutations in the chloroplast genome was significantly slower, and we detected no signal of relaxed purifying selection in the younger selfing lineage (Fig. 4b; Table 1). To our knowledge, there has been no explicit comparison of nuclear vs chloroplast genes associated with mating system transitions, although a few studies have detected similar (Wang *et al.*, 2021) or weak (Glémin & Muyle, 2014) signatures of relaxed selection in the chloroplast genomes of selfers. The slower rate of accumulation of deleterious mutations for chloroplast genes can probably be explained by the smaller reduction in N_e and reduced sensitivity to hitchhiking effects in comparison with nuclear genes (Glémin & Muyle, 2014).

Evolution of morphological selfing syndromes

In contrast to the limited investigation of the genomic selfing syndrome, numerous studies on diverse taxa have documented changes in morphological and functional features of flowers associated with evolutionary transition from outcrossing to selfing (reviewed in Sicard & Lenhard, 2011; Tsuchimatsu &

© 2024 The Authors
New Phytologist © 2024 New Phytologist Foundation

14698137, 0, Downloaded from https://nph.onlinelibrary.wiley.com/doi/10.1111/nph.19522 by Peking University Health, Wiley Online Library on [15/01/2024]. See the Terms and Conditions (https://onlinelibrary.wiley.com/terms-and-conditions) on Wiley Online Library for rules of use; OA articles are governed by the applicable Creative Commons License

Fujii, 2022). The shift to selfing can be initiated by different floral mechanisms, including the loss of herkogamy (e.g. *Eichhornia paniculata*, Vallejo-Marín & Barrett, 2009), dichogamy (e.g. *Collinsia* spp. Kalisz *et al.*, 2012), and self-incompatibility (e.g. *Capsella rubella*, Sicard *et al.*, 2011). Genetic modifications to these reproductive traits, if accompanied by increased selfing, are usually followed by changes in other floral traits (e.g. reduced flower size, pollen, and nectar production), which further promote the evolution of the morphological selfing syndrome.

However, such changes are not an inevitable outcome of transitions to selfing, as is evident in North American populations of *Arabidopsis lyrata* in which a recent shift to selfing caused by the loss of self-incompatibility has not been accompanied by changes to flower size (Hoebe *et al.*, 2009). Because ancestral distylous populations are fully self and intra-morph compatible (Yuan *et al.*, 2017), the transition to selfing in *P. oreodoxa* is not initiated by the loss of self-incompatibility. Rather, the loss of well-developed herkogamy appears to be the key reproductive trait influencing changes to the mating system of populations (Yuan *et al.*, 2023), as is also the case in numerous other angiosperm species (Opedal, 2018). Although there was evidence in both young and old selfing lineages of *P. oreodoxa* for modifications to morphological traits, consistent with the evolution of selfing syndrome, nearly all of the changes were less well-developed in the younger selfing lineage compared with the old selfing lineage (Fig. 5), as predicted given the different timescales since the origins of selfing in the two lineages.

Decomposition of the genetic basis of individual and correlated components of the morphological selfing syndrome, and whether traits have evolved independently, has rarely been attempted. However, recent studies of the selfing syndrome of *Ipomoea lacunosa* demonstrated using Q_{st}–F_{st} comparisons (Rifkin *et al.*, 2019) and quantitative trait locus (QTL)-mapping (Liao *et al.*, 2022) that modifications to flower size and nectar traits reflected directional selection on at least two independent evolutionary modules. Quantitative trait locus mapping in *Mimulus* (Fishman *et al.*, 2002) and *Capsella* (Slotte *et al.*, 2012) indicate that most of traits associated with selfing (e.g. flower size and stigma-anther separation) have likely evolved gradually by the sequential fixation of small-effect alleles, although in some cases major-effect loci can be involved (e.g. reduction of pollen number in *Arabidopsis thaliana*, Tsuchimatsu *et al.*, 2020).

In our study, it seems probable that the cascade of morphological changes accompanying the transition to selfing were initiated by a major effect mutation at the CYP^T locus (Huu *et al.*, 2016; Mora-Carrera *et al.*, 2023). This change was likely followed by more gradual adaptive evolution of sex allocation based on polygenic variation, given the substantial phenotypic variation among populations and lineages in selfing traits (Fig. 5). However, at this stage, we cannot rule out the role of genetic drift in contributing to these changes. Moreover, assuming selection does indeed play a primary role, it is also unclear what the tempo of response to selection might be on the quantitative floral traits comprising the selfing syndrome as this will depend, in part, on the standing genetic variation of these traits.

Existing models for inferring adaptive evolution often assume idealized random mating in populations. However, Noël *et al.* (2017) used experimental evolution to compare the response of quantitative genetic selection on a morphological trait in selfing vs outcrossing populations of the freshwater hermaphrodite snail *Physa acuta*. Their experiments revealed that in selfing populations, there was an initially fast response to selection, but this rapidly slowed. Their findings of short-term positive response but longer term negative effects of selfing on adaptive evolution may help to explain the initial changes evident for morphological traits in the younger selfing lineage of *P. oreodoxa*. Subsequent trait changes might be slower to occur because of low genetic variation arising from severe bottlenecks. Also further trait change may influence pollinator service and compromise any adaptive benefits that arise from maintaining low levels of outcrossing, although visitation already occurs at very low levels in homostylous populations (Yuan *et al.*, 2023; Fig. 2). The extent to which drift vs selection might drive subsequent morphological changes during a shift from mixed mating to predominant selfing requires further studies.

Conclusions

Our study represents a comprehensive analysis of the evolutionary history of the morphological and genomic selfing syndromes. The occurrence of independently evolved selfing lineages of different ages facilitated this comparison and demonstrated parallel development of morphological and genomic changes to different degrees, probably depending on the history of selfing. Compared with other model systems (e.g. *Arabidopsis* and *Capsella*) used for studies of mating-system transitions (reviewed in Mattila *et al.*, 2020), *Primula* provides an unusual opportunity for further comparative analyses because the genus is composed of numerous independent transitions from outcrossing to selfing (de Vos *et al.*, 2014; Zhong *et al.*, 2019), including relatively old and young selfing lineages (Wang *et al.*, 2021). This floral and mating system diversity should be exploited for future comparative investigations of the evolution of morphological and genomic features of selfing syndromes.

Acknowledgements

This research was supported by the Strategic Priority Research Program of the Chinese Academy of Sciences (XDB31000000) to D-ZL, the National Natural Science Foundation of China (31971394) to WZ, the Key Basic Research Program of Yunnan Province (202201AS070057, 202101 BC070003, and 202103 AC100003) to WZ, and a Discovery Grant (RGPIN/06442-2017) from the Natural Sciences and Engineering Research Council of Canada to SCHB.

Competing interests

None declared.

© 2024 The Authors
New Phytologist © 2024 New Phytologist Foundation

14698137, 0, Downloaded from https://nph.onlinelibrary.wiley.com/doi/10.1111/nph.19522 by Peking University Health, Wiley Online Library on [15/01/2024]. See the Terms and Conditions (https://onlinelibrary.wiley.com/terms-and-conditions) on Wiley Online Library for rules of use; OA articles are governed by the applicable Creative Commons License

Author contributions

WZ, SCHB and D-ZL planned and designed the research. Z-HZ, WZ, H-YS, XW, HW, LZ and Z-KW performed experiments and conducted fieldwork. Z-HZ and WZ analyzed the data. WZ, SCHB and Z-HZ wrote the manuscript.

ORCID

Spencer C. H. Barrett https://orcid.org/0000-0002-7762-3455
De-Zhu Li https://orcid.org/0000-0002-4990-724X
Hong Wang https://orcid.org/0000-0003-2618-0196
Zhi-Hua Zeng https://orcid.org/0000-0002-3601-3618
Li Zhong https://orcid.org/0000-0001-7776-5042
Wei Zhou https://orcid.org/0000-0001-5527-3776

Data availability

Plastid genome assembles are deposited in GenBank database with accession nos. provided in Table S4. RNA-seq data are deposited in the National Genomic Data Center of the China National Center for Bioinformation (GSA: CRA012426).

References

Akashi H, Osada N, Ohta T. 2012. Weak selection and protein evolution. *Genetics* **192**: 15–31.

Arunkumar R, Ness RW, Wright SI, Barrett SCH. 2015. The evolution of selfing is accompanied by reduced efficacy of selection and purging of deleterious mutations. *Genetics* **199**: 817–829.

Barrett SCH. 1992. Heterostylous genetic polymorphisms: model systems for evolutionary analysis. In: Barrett SCH, ed. *Evolution and function of heterostyly.* Berlin, Germany: Springer, 1–29.

Barrett SCH. 2019. 'A most complex marriage arrangement': recent advances on heterostyly and unresolved questions. *New Phytologist* **224**: 1051–1067.

Barrett SCH, Arunkumar R, Wright SI. 2014. The demography and population genomics of evolutionary transitions to self-fertilization in plants. *Philosophical Transactions of the Royal Society, B: Biological Sciences* **369**: 20130344.

Beaumont MA, Zhang WY, Balding DJ. 2002. Approximate Bayesian computation in population genetics. *Genetics* **162**: 2025–2035.

Brandvain Y, Wright SI. 2016. The limits of natural selection in a nonequilibrium world. *Trends in Genetics* **32**: 201–210.

Charlesworth D, Charlesworth B. 1979. A model for the evolution of distyly. *American Naturalist* **114**: 467–498.

Charlesworth D, Wright SI. 2001. Breeding systems and genome evolution. *Current Opinion in Genetics and Development* **11**: 685–690.

Chen J, Glémin S, Lascoux M. 2017. Genetic diversity and the efficacy of purifying selection across plant and animal species. *Molecular Biology and Evolution* **34**: 1417–1428.

Cornuet JM, Santos F, Beaumont MA, Robert CP, Marin JM, Balding DJ, Guillemaud T, Estoup A. 2008. Inferring population history with DIY ABC: a user-friendly approach to approximate Bayesian computation. *Bioinformatics* **24**: 2713–2719.

Crosby JL. 1949. Selection of an unfavourable gene-complex. *Evolution* **3**: 212–230.

Cutter AD. 2019. Reproductive transitions in plants and animals: selfing syndrome, sexual selection and speciation. *New Phytologist* **224**: 1080–1094.

Darriba D, Posada D, Kozlov AM, Stamatakis A, Morel B, Flouri T. 2020. ModelTest-NG: a new and scalable tool for the selection of DNA and protein evolutionary models. *Molecular Biology and Evolution* **37**: 291–294.

Darwin C. 1877. *The different forms of flowers on plants of the same species.* London, UK: John Murray.

David P, Pujol B, Viard F, Castella V, Goudet J. 2007. Reliable selfing rate estimates from imperfect population genetic data. *Molecular Ecology* **16**: 2474–2487.

Doyle J. 1991. DNA protocols for plants: CTAB total DNA isolation. In: Hewitt GM, Johnston AWB, Young JPW, eds. *Molecular techniques in taxonomy.* Berlin, Germany: Springer, 283–293.

Escobar JS, Cenci A, Bolognini J, Haudry A, Laurent S, David J, Glémin S. 2010. An integrative test of the dead-end hypothesis of selfing evolution in Triticeae (Poaceae). *Evolution* **64**: 2855–2872.

Felsenstein J. 2005. *PHYLIP (phylogeny inference package) v.3.6.* Seattle, WA, USA: Department of Genome Sciences, University of Washington.

Fishman L, Kelly AJ, Willis JH. 2002. Minor quantitative trait loci underlie floral traits associated with mating system divergence in *Mimulus. Evolution* **56**: 2138–2155.

Fornoni J, Ordano M, Pérez-Ishiwara R, Boege K, Domínguez CA. 2015. A comparison of floral integration between selfing and outcrossing species: a meta-analysis. *Annals of Botany* **117**: 299–306.

Foxe JP, Slotte T, Stahl EA, Neuffer B, Hurka H, Wright SI. 2009. Recent speciation associated with the evolution of selfing in *Capsella. Proceedings of the National Academy of Sciences, USA* **106**: 5241–5245.

Ganders FR. 1979. The biology of heterostyly. *New Zealand Journal of Botany* **17**: 607–635.

Ganders FR, Denny SK, Tsai D. 1985. Breeding systems and genetic variation in *Amsinckia spectabilis* (Boraginaceae). *Canadian Journal of Botany* **63**: 533–538.

Gao H, Williamson S, Bustamante CD. 2007. A Markov chain Monte Carlo approach for joint inference of population structure and inbreeding rates from multilocus genotype data. *Genetics* **176**: 1635–1651.

Glémin S, Galtier N. 2012. Genome evolution in outcrossing versus selfing versus asexual species. In: Anisimova M, ed. *Evolutionary genomics: statistical and computational methods.* Totowa, NJ, USA: Humana Press, 311–335.

Glémin S, Muyle A. 2014. Mating systems and selection efficacy: a test using chloroplastic sequence data in Angiosperms. *Journal of Evolutionary Biology* **27**: 1386–1399.

Glémin S, Ronfort J. 2013. Adaptation and maladaptation in selfing and outcrossing species: new mutations versus standing variation. *Evolution* **67**: 225–240.

Guo YL, Bechsgaard JS, Slotte T, Neuffer B, Lascoux M, Weigel D, Schierup MH. 2009. Recent speciation of *Capsella rubella* from *Capsella grandiflora*, associated with loss of self-incompatibility and an extreme bottleneck. *Proceedings of the National Academy of Sciences, USA* **106**: 5246–5251.

Hoebe PN, Stift M, Tedder A, Mable BK. 2009. Multiple losses of self-incompatibility in North-American *Arabidopsis lyrata*?: phylogeographic context and population genetic consequences. *Molecular Ecology* **18**: 4924–4939.

Huu CN, Kappel C, Keller B, Sicard A, Takebayashi Y, Breuninger H, Nowak MD, Bäurle I, Himmelbach A, Burkart M *et al.* 2016. Presence versus absence of *CYP734A50* underlies the style-length dimorphism in primroses. *eLife* **5**: e17956.

Igic B, Busch JW. 2013. Is self-fertilization an evolutionary dead end? *New Phytologist* **198**: 386–397.

Kalisz S, Randle A, Chaiffetz D, Faigeles M, Butera A, Beight C. 2012. Dichogamy correlates with outcrossing rate and defines the selfing syndrome in the mixed-mating genus *Collinsia. Annals of Botany* **109**: 571–582.

Kamran-Disfani A, Agrawal AF. 2014. Selfing, adaptation and background selection in finite populations. *Journal of Evolutionary Biology* **27**: 1360–1371.

Kappel C, Huu CN, Lenhard M. 2017. A short story gets longer: recent insights into the molecular basis of heterostyly. *Journal of Experimental Botany* **68**: 5719–5730.

Katoh K, Standley DM. 2013. Mafft multiple sequence alignment software v.7: improvements in performance and usability. *Molecular Biology and Evolution* **30**: 772–780.

Kopelman NM, Mayzel J, Jakobsson M, Rosenberg NA, Mayrose I. 2015. Clumpak: a program for identifying clustering modes and packaging population structure inferences across *K. Molecular Ecology Resources* **15**: 1179–1191.

© 2024 The Authors
New Phytologist © 2024 New Phytologist Foundation

14698137, 0, Downloaded from https://nph.onlinelibrary.wiley.com/doi/10.1111/nph.19522 by Peking University Health, Wiley Online Library on [15/01/2024]. See the Terms and Conditions (https://onlinelibrary.wiley.com/terms-and-conditions) on Wiley Online Library for rules of use; OA articles are governed by the applicable Creative Commons License

Laenen B, Tedder A, Nowak MD, Toräng P, Wunder J, Wötzel S, Steige KA, Kourmpetis Y, Odong T, Drouzas AD *et al.* 2018. Demography and mating system shape the genome-wide impact of purifying selection in *Arabis alpina*. *Proceedings of the National Academy of Sciences, USA* **115**: 816–821.

Liao IT, Rifkin JL, Cao G, Rausher MD. 2022. Modularity and selection of floral traits in the evolution of the selfing syndrome in *Ipomoea lacunosa* (Convulvulaceae). *New Phytologist* **233**: 1505–1519.

Lloyd DG. 1965. Evolution of self-compatibility and racial differentiation in *Leavenworthia*. (Cruciferae). *Contributions from the Gray Herbarium of Harvard University* **195**: 3–134.

Mast AR, Kelso S, Conti E. 2006. Are any primroses (*Primula*) primitively monomorphic? *New Phytologist* **171**: 605–616.

Mattila TM, Laenen B, Slotte T. 2020. Population genomics of transitions to selfing in Brassicaceae model systems. In: Dutheil JY, ed. *Statistical population genomics*. New York, NY, USA: Springer, 269–288.

McDonald JH, Kreitman M. 1991. Adaptive protein evolution at the *Adh* locus in *Drosophila*. *Nature* **351**: 652–654.

Mora-Carrera E, Stubbs RL, Keller B, Léveillé-Bourret É, de Vos JM, Szövényi P, Conti E. 2023. Different molecular changes underlie the same phenotypic transition: origins and consequences of independent shifts to homostyly within species. *Molecular Ecology* **32**: 61–78.

Morgan MT, Barrett SCH. 1989. Reproductive correlates of mating system evolution in *Eichhornia paniculata* (Spreng.) Solms (Pontederiaceae). *Journal of Evolutionary Biology* **2**: 183–203.

Nei M. 1987. *Molecular evolutionary genetics*. New York, NY, USA: Columbia University Press.

Ness RW, Siol M, Barrett SCH. 2012. Genomic consequences of transitions from cross- to self-fertilization on the efficacy of selection in three independently derived selfing plants. *BMC Genomics* **13**: 1–12.

Noël E, Jarne P, Glémin S, MacKenzie A, Segard A, Sarda V, David P. 2017. Experimental evidence for the negative effects of self-fertilization on the adaptive potential of populations. *Current Biology* **27**: 237–242.

Ohta T. 1992. The nearly neutral theory of molecular evolution. *Annual Review of Ecology and Systematics* **23**: 263–286.

Opedal ØH. 2018. Herkogamy, a principal functional trait of plant reproductive biology. *International Journal of Plant Sciences* **179**: 677–687.

Peakall R, Smouse PE. 2006. GENALEX 6: genetic analysis in Excel. Population genetic software for teaching and research. *Molecular Ecology Notes* **6**: 288–295.

Piper JG, Charlesworth B, Charlesworth D. 1984. A high rate of self-fertilization and increased seed fertility of homostyle primroses. *Nature* **310**: 50–51.

Pritchard JK, Stephens M, Donnelly P. 2000. Inference of population structure using multilocus genotype data. *Genetics* **155**: 945–959.

Purcell S, Neale B, Todd-Brown K, Thomas L, Ferreira MAR, Bender D, Maller J, Sklar P, de Bakker PIW, Daly MJ *et al.* 2007. PLINK: a tool set for whole-genome association and population-based linkage analyses. *American Journal of Human Genetics* **81**: 559–575.

R Core Team. 2021. *R: a language and environment for statistical computing*. Vienna, Austria: R Foundation for Statistical Computing. [WWW document] URL https://www.r-project.org/ [accessed 2 October 2021].

Raj A, Stephens M, Pritchard JK. 2014. fastSTRUCTURE: variational inference of population structure in large SNP data sets. *Genetics* **197**: 573–589.

Rand DM, Kann LM. 1996. Excess amino acid polymorphism in mitochondrial DNA: contrasts among genes from *Drosophila*, mice, and humans. *Molecular Biology and Evolution* **13**: 735–748.

Richards AJ. 2003. *Primula*. Portland, OR, USA: Timber Press.

Rifkin JL, Liao IT, Castillo AS, Rausher MD. 2019. Multiple aspects of the selfing syndrome of the morning glory *Ipomoea lacunosa* evolved in response to selection: a Q_{st}–F_{st} comparison. *Ecology and Evolution* **9**: 7712–7725.

Ritland C, Ritland K. 1989. Variation of sex allocation among eight taxa of the *Mimulus guttatus* species complex (Scrophulariaceae). *American Journal of Botany* **76**: 1731–1739.

Ronquist F, Huelsenbeck JP. 2003. MRBAYES 3: bayesian phylogenetic inference under mixed models. *Bioinformatics* **19**: 1572–1574.

Rozas J, Ferrer-Mata A, Sánchez-DelBarrio JC, Guirao-Rico S, Librado P, Ramos-Onsins SE, Sánchez-Gracia A. 2017. DNASP 6: DNA sequence polymorphism analysis of large data sets. *Molecular Biology and Evolution* **34**: 3299–3302.

Schneider A, Charlesworth B, Eyre-Walker A, Keightley PD. 2011. A method for inferring the rate of occurrence and fitness effects of advantageous mutations. *Genetics* **189**: 1427–1437.

Shao JW, Wang HF, Fang SP, Conti E, Chen YJ, Zhu HM. 2019. Intraspecific variation of self-incompatibility in the distylous plant *Primula merrilliana*. *AoB Plants* **11**: plz030.

Shimizu KK, Tsuchimatsu T. 2015. Evolution of selfing: recurrent patterns in molecular adaptation. *Annual Review of Ecology, Evolution, and Systematics* **46**: 593–622.

Sicard A, Lenhard M. 2011. The selfing syndrome: a model for studying the genetic and evolutionary basis of morphological adaptation in plants. *Annals of Botany* **107**: 1433–1443.

Sicard A, Stacey N, Hermann K, Dessoly J, Neuffer B, Bäurle I, Lenhard M. 2011. Genetics, evolution, and adaptive significance of the selfing syndrome in the genus *Capsella*. *Plant Cell* **23**: 3156–3171.

Slotte T, Hazzouri KM, Ågren JA, Koenig D, Maumus F, Guo YL, Steige K, Platts AE, Escobar JS, Newman LK *et al.* 2013. The *Capsella rubella* genome and the genomic consequences of rapid mating system evolution. *Nature Genetics* **45**: 831–835.

Slotte T, Hazzouri KM, Stern DL, Andolfatto P, Wright SI. 2012. Genetic architecture and adaptive significance of the selfing syndrome in *Capsella*. *Evolution* **66**: 1360–1374.

Stamatakis A. 2014. RAxML v.8: a tool for phylogenetic analysis and post-analysis of large phylogenies. *Bioinformatics* **30**: 1312–1313.

Stebbins GL. 1957. Self fertilization and population variability in the higher plants. *American Naturalist* **91**: 337–354.

Takebayashi N, Morrell PL. 2001. Is self-fertilization an evolutionary dead end? Revisiting an old hypothesis with genetic theories and a macroevolutionary approach. *American Journal of Botany* **88**: 1143–1150.

Tsuchimatsu T, Fujii S. 2022. The selfing syndrome and beyond: diverse evolutionary consequences of mating system transitions in plants. *Philosophical Transactions of the Royal Society B* **377**: 20200510.

Tsuchimatsu T, Kakui H, Yamazaki M, Marona C, Tsutsui H, Hedhly A, Meng D, Sato Y, Städler T, Grossniklaus U *et al.* 2020. Adaptive reduction of male gamete number in the selfing plant *Arabidopsis thaliana*. *Nature Communications* **11**: 2885.

Vallejo-Marín M, Barrett SCH. 2009. Modification of flower architecture during early stages in the evolution of self-fertilization. *Annals of Botany* **103**: 951–962.

Vaser R, Adusumalli S, Leng SN, Sikic M, Ng PC. 2016. SIFT missense predictions for genomes. *Nature Protocols* **11**: 1–9.

de Vos JM, Keller B, Zhang LR, Nowak MD, Conti E. 2018. Mixed mating in homostylous species: genetic and experimental evidence from an alpine plant with variable herkogamy, *Primula halleri*. *International Journal of Plant Sciences* **179**: 87–99.

de Vos JM, Wüest RO, Conti E. 2014. Small and ugly? Phylogenetic analyses of the "selfing syndrome" reveal complex evolutionary fates of monomorphic primrose flowers. *Evolution* **68**: 1042–1057.

Wang J, El-Kassaby YA, Ritland K. 2012. Estimating selfing rates from reconstructed pedigrees using multilocus genotype data. *Molecular Ecology* **21**: 100–116.

Wang XJ, Barrett SCH, Zhong L, Wu ZK, Li DZ, Wang H, Zhou W. 2021. The genomic selfing syndrome accompanies the evolutionary breakdown of heterostyly. *Molecular Biology and Evolution* **38**: 168–180.

Wright SI, Kalisz S, Slotte T. 2013. Evolutionary consequences of self-fertilization in plants. *Proceedings of the Royal Society: Biological Sciences* **280**: 2013013.

Wright SI, Ness RW, Foxe JP, Barrett SCH. 2008. Genomic consequences of outcrossing and selfing in plants. *International Journal of Plant Sciences* **169**: 105–118.

Yi HQ, Wang JY, Wang J, Rausher MD, Kang M. 2022. Genomic insights into inter-and intraspecific mating system shifts in *Primulina*. *Molecular Ecology* **31**: 5699–5713.

Yuan S, Barrett SCH, Duan TT, Qian X, Shi MM, Zhang DX. 2017. Ecological correlates and genetic consequences of evolutionary transitions from distyly to homostyly. *Annals of Botany* **120**: 775–789.

© 2024 The Authors
New Phytologist © 2024 New Phytologist Foundation

14698137, 0, Downloaded from https://nph.onlinelibrary.wiley.com/doi/10.1111/nph.19522 by Peking University Health, Wiley Online Library on [15/01/2024]. See the Terms and Conditions (https://onlinelibrary.wiley.com/terms-and-conditions) on Wiley Online Library for rules of use; OA articles are governed by the applicable Creative Commons License

Yuan S, Barrett SCH, Li CH, Li XJ, Xie KP, Zhang DX. 2019. Genetics of distyly and homostyly in a self-compatible *Primula*. *Heredity* **122**: 110–119.

Yuan S, Zeng G, Zhang DX. 2018. Development of microsatellite markers for *Primula oreodoxa* (Primulaceae), a distylous-homostylous species. *Applications in Plant Sciences* **6**: e01150.

Yuan S, Zeng G, Zhang K, Wu MS, Zhang DX, Harder LD, Barrett SCH. 2023. Diverse mating consequences of the evolutionary breakdown of the sexual polymorphism heterostyly. *Proceedings of the National Academy of Sciences, USA* **120**: e2214492120.

Zeng G, Barrett SCH, Yuan S, Zhang DX. 2022. Evolutionary breakdown of distyly to homostyly is accompanied by reductions in floral scent in *Primula oreodoxa*. *Journal of Systematics and Evolution* **61**: 518–529.

Zhang W, Hu YF, He X, Zhou W, Shao JW. 2021. Evolution of autonomous selfing in marginal habitats: spatiotemporal variation in the floral traits of the distylous *Primula wannanensis*. *Frontiers in Plant Science* **12**: 781281.

Zhang Z, Kryvokhyzha D, Orussci M, Glémin S, Milesi P, Lascoux M. 2022. How broad is the selfing syndrome? Insights from convergent evolution of gene expression across species and tissues in the *Capsella* genus. *New Phytologist* **236**: 2344–2357.

Zhong L, Barrett SCH, Wang XJ, Wu ZK, Sun HY, Li DZ, Wang H, Zhou W. 2019. Phylogenomic analysis reveals multiple evolutionary origins of selfing from outcrossing in a lineage of heterostylous plants. *New Phytologist* **224**: 1290–1303.

Zhou W, Barrett SCH, Li HD, Wu ZK, Wang XJ, Wang H, Li DZ. 2017. Phylogeographic insights on the evolutionary breakdown of heterostyly. *New Phytologist* **214**: 1368–1380.

Supporting Information

Additional Supporting Information may be found online in the Supporting Information section at the end of the article.

Fig. S1 Models that were tested for lineage differentiation history of the *Primula oreodoxa* complex using Approximate Bayesian Computation modeling.

Fig. S2 Correlation analysis of 20 phenotypic traits in the *Primula oreodoxa* complex.

Fig. S3 Unfolded synonymous and nonsynonymous site frequency spectra of each identified lineage of the *Primula oreodoxa* complex.

Fig. S4 Total number of flowers sampled and measured from populations in the *Primula oreodoxa* complex.

Methods S1 Detailed information regarding molecular and morphological data preprocessing.

Table S1 Geographical locations of populations of the *Primula oreodoxa* complex investigated in this study.

Table S2 Sixteen pairs of microsatellite primer information for the *Primula oreodoxa* complex.

Table S3 Trait values for the three identified lineages of the *Primula oreodoxa* complex.

Table S4 Features of the plastid genome of the sequenced plants of the *Primula oreodoxa* complex in this study.

Table S5 Posterior distribution of parameters for the best fitting lineage differentiation model of the *Primula oreodoxa* complex.

Please note: Wiley is not responsible for the content or functionality of any Supporting Information supplied by the authors. Any queries (other than missing material) should be directed to the *New Phytologist* Central Office.

© 2024 The Authors
New Phytologist © 2024 New Phytologist Foundation

14698137, 0, Downloaded from https://nph.onlinelibrary.wiley.com/doi/10.1111/nph.19522 by Peking University Health, Wiley Online Library on [15/01/2024]. See the Terms and Conditions (https://onlinelibrary.wiley.com/terms-and-conditions) on Wiley Online Library for rules of use; OA articles are governed by the applicable Creative Commons License